Pure & Appl. Chem., Vol. 61, No. 6, pp. 1001–1007, 1989.
Printed in Great Britain.

Thermodynamics of gas–surface interactions

Gerhard Ertl

Fritz-Haber-Institut der Max-Planck-Gesellschaft, Faradayweg 4-6,
D-1000 Berlin 33, W. Germany

Abstract - The development of a large variety of surface spectroscopic methods enables microscopic characterisation of the species adsorbed on well-defined single crystal surfaces which supplements measurements of macroscopic thermodynamic properties of gas-solid equilibria. A series of examples with chemisorbed and physisorbed systems serves to illustrate the underlying principles.

INTRODUCTION

The equilibrium between gaseous particles and a solid surface can be described by a function $\Theta(p,T)$, where Θ is the surface concentration or coverage of the adsorbed species, p the partial pressure and T the temperature. This equilibrium is governed by the interactions of the adparticles with the surface and by the interactions between the adsorbed species. Traditionally, one distinguishes between weak (= physisorption) and strong (= chemisorption) adsorption, whereby an adsorption energy of 40 kJ/mol can be considered as a rough borderline. 'Real' surfaces are polycrystalline and are hence a priori energetically heterogeneous. Fundamental processes are therefore preferably studied with well-defined single crystal surfaces which can be prepared under ultra high vacuum (UHV) conditions and characterized by a variety of modern surface spectroscopic methods (ref. 1). This contribution will be restricted to model systems of this type. The possibility of atomic-scale characterisation of these systems enables also the investigation of microscopic properties and provides direct access to concepts of statistical thermodynamics.

Phenomenological thermodynamic quantities such as heats or entropies of adsorption may be derived experimentally either from calorimetric measurements or through analysis of the recorded function $\Theta(p,T)$.

Calorimetric techniques require a minimum surface area in order to achieve a sufficiently high signal to noise ratio and can therefore not routinely be applied to single crystal samples with surface areas typically < 1 cm^2. No such restriction holds for analysis of adsorption isotherms or isosteres, provided that a sensitive enough probe for the coverage is available. This can be realized in various ways as will become evident from some of the examples to be presented below.

It is customary in single crystal studies to define the absolute coverage Θ as the ratio of density of adsorbed particles over the density of substrate atoms in the topmost layer. Saturation of the (first) adlayer occurs at Θ_{max} which will generally be unequal to 1. The relative coverage $\vartheta = \Theta/\Theta_{max}$, on the other hand, runs up to unity at monolayer saturation and corresponds to the commonly used notation, defined as the fraction of the surface area covered by the adsorbate (ref. 2).

CHEMISORPTION

The termination of the bulk lattice of the surface of a solid can be considered as a source of unsaturated valencies which are able to form regular chemical bonds with suitable partners arriving from the gas phase. The simplest form of the interaction potential along the surface normal (disregarding possible dissociation or the presence of an 'intrinsic' precursor state) is illustrated schematically by fig. 1a, while fig. 1b represents the periodic variation of the potential in a direction parallel to the surface due to the periodic arrangements of atoms in a single crystal surface. This situation resembles closely the model underlying the derivation of the famous Langmuir adsorption isotherm: "The surface of crystals resembles to some extent a checkerboard. When molecules of gas are adsorbed by such a surface these molecules take up definite positions with respect to the surface lattice and thus tend to form a new lattice above the old" (ref. 3).

Figure 2 shows an adsorption isotherm $\vartheta(p)$ at T = const. for CO adsorbed on a Pd(111) surface (ref. 4), together with different attempts to fit the data with a Langmuir isotherm, $\vartheta = bp/(1 + bp)$, by varying the adjustable parameter b. It is obviously not possible to find satisfying agreement with the experimental data. An additional problem arises with respect to the absolute maximum coverage

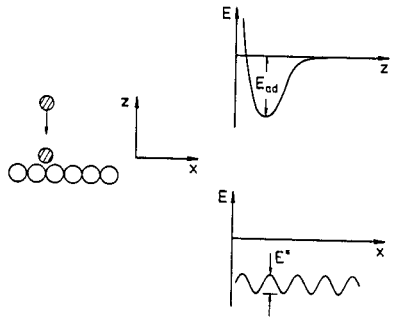

Fig. 1: Schematic interaction potential between a gaseous particle and a single crystal surface.

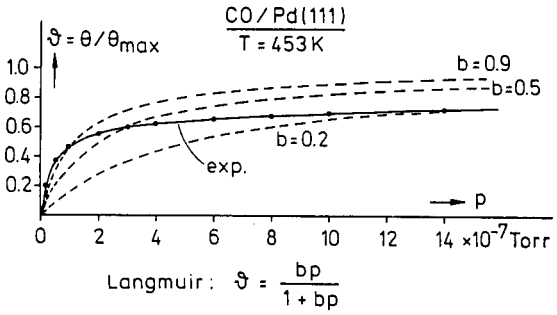

Fig. 2: Adsorption isotherm for adsorption of CO on a Pd(111) surface at 453 K (full line) and several attempts to fit the experimental data with a Langmuir isotherm (dashed lines).

Θ_{max}: While with the Langmuir model necessarily $\Theta_{max} = 1$ (i.e. each adsorption site being determined by the substrate lattice is occupied), the actual saturation coverage is only about 0.7! Derivation of the isosteric differential heat of adsorption from a series of isotherms recorded at different temperatures as a function of Θ (fig. 3) demonstrates further the invalidity of the concepts underlying the Langmuir isotherm: Instead of being independent of coverage, the adsorption energy remains constant only up to $\Theta = 1/3$, then it drops suddenly and then starts to decrease markedly around $\Theta = 1/2$, signaling the approach of saturation. The solution of this apparent discrepancy has to be sought in the operation of (essentially repulsive) interactions between the adsorbed particles whose existence is completely neglected in the derivation of the Langmuir isotherm, and which manifest themselves also in the structures of the various ordered phases as determined by low energy electron diffraction (LEED) and vibrational spectroscopy (ref. 4,5): Up to $\Theta = 1/3$ the CO molecules occupy threefold coordinated adsorption sites leading to a $\sqrt{3}x\sqrt{3}R30°$ superstructure at $\Theta = 1/3$ (fig. 4a). Beyond this coverage the unit cell of the overlayer starts to become continuously compressed whereby part of the adsorbed particles is displaced from their original sites (hence the sudden drop of the adsorption energy by about 8 kJ/mol), until at $\Theta = 1/2$ a c4x2 structure is formed in which the adsorbed molecules are now all in twofold coordinated (bridge) sites (fig. 4b). At even higher coverages, incommensurate structures (figs. 4c,d) appear in which the configuration of the adsorbate approaches close-packed structures as determined by the effective diameter of the adparticle which finally also determines the saturation coverage.

There exists still another shortcoming of the Langmuir model: It assumes infinitely high activation barriers between neighboring adsorption sites (giving rise to 'immobile' adsorption even under conditions for which the adsorption-desorption equilibrium is established), while in fact these barriers are roughly one order of magnitude smaller than the adsorption energy (ref. 6) giving rise to appreciable mobility within the adlayer.

The existence of high surface mobility during the adsorption/desorption equilibrium manifests itself for example in the adsorption entropy: Fig. 5 shows the differential entropy of adsorption as a function of coverage (as derived form a set of adsorption isotherms) for the system CO/Pd(100) at 410 K together with calculated data for the limiting cases of completely localized and delocalized layers (ref. 7). Up to $\Theta \approx 0.35$ the experimental data are between those predicted by both models. Above this coverage, however, S_{ad} decreases even more rapidly with Θ than predicted by the model of localized, but random adsorption. This is due to a higher degree of order within the adlayer which in turn is a consequence of the operation of interactions between the adsorbed particles playing an increasing role at decreasing mutual distances, i.e. increasing coverage.

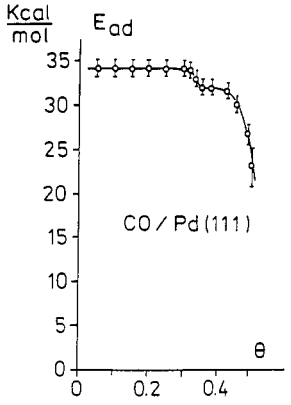

Fig. 3: Isosteric heat of adsorption for CO on a Pd(111) surfaces as a function of coverage.

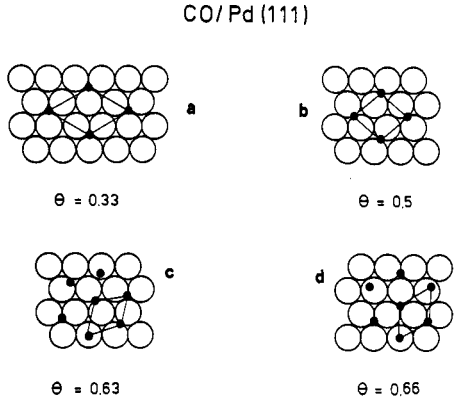

Fig. 4: Structure models for CO adsorbed on Pt(111) at various coverages.

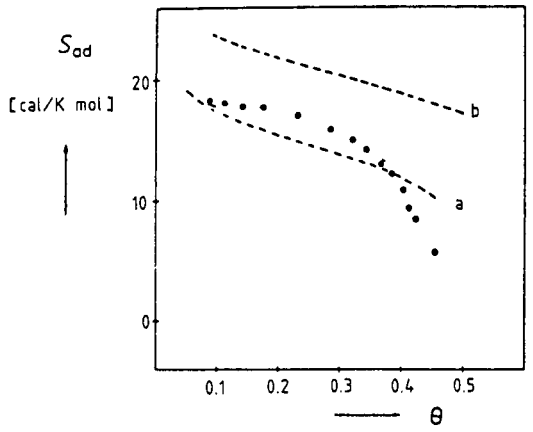

Fig. 5: Differential entropy of adsorption for CO on Pd(100) at 410 K as a function of coverage (dots). Dashed lines: Theoretical data for models of localized (a) and delocalized adsorption (b).

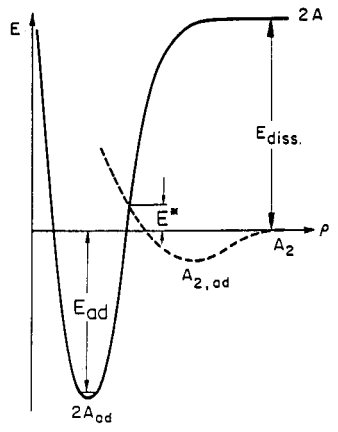

Fig. 6: Schematic Lennard-Jones potential diagram illustrating the progress of dissociative chemisorption.

The interactions between adsorbed particles may be 'direct' (like dipole-dipole or van der Waals type) or 'indirect', i.e. mediated throug the valence electrons of the substrate in a similar manner as the 'through bond' interaction in organic molecules. The latter are of particular relevance for systems involving strongly bound atomic adsorbates, such as H or O, and may be repulsive as well as attractive (ref. 8). The formation of such overlayers through interaction with the molecular gaseous species can be rationalized in terms of the well-known, one-dimensional Lennard-Jones potential (fig. 6). the strength of the surface-adsorbate bond, $E_{S\text{-}A}$, is related with the adsorption energy, E_{ad}, and the dissociation energy of the free molecule, E_{diss}, through $E_{S\text{-}A} = \frac{1}{2}(E_{ad} + E_{diss})$. The gas-surface equilibrium is determined by E_{ad}, while the activation energy E^* affects solely the kinetics (= sticking coefficient). If the temperature is low enough, the rate of desorption becomes negligible. Once a certain coverage has been reached, the gas flow to the surface may be turned off, and we are now left with equilibrium formation within the adlayer without taking the gas phase into account.

In contrast to the examples of CO adsorption presented above, 'small' adsorbates such as H frequently occupy identical adsorption sites irrespective of coverage as determined by the substrate lattice structure and represent thus two-dimensional lattice-gas systems.

Fig. 7 shows two structures formed in the system H/Fe(110) at coverages $\Theta = \frac{1}{2}$ and $\Theta = \frac{2}{3}$ (ref. 9). Saturation is reached at $\Theta = 1$ when all identical desorption sites are occupied. The (equilibrium) degree of long-range order within the shown structures depends on temperature and coverage; order-disorder transitions can be followed by LEED. The experimentally determined phase diagram is reproduced in fig. 8a which shows that above critical temperatures T = 245 and 265 K, respectively, long-range order no longer exists. This effect has to be attributed to the competition between the interaction energies between the adparticles and the thermal energy. Theoretical modelling of this phase diagram could be successfully achieved (fig. 8b) by adjusting a set of four interaction parameters whose strength is throughout <8 kJ/mol, which is very small if compared with the ~250 kJ/mol of the H-surface bond energy (ref. 10). This example demonstrates how very subtle energetic effects may manifest themselves experimentally and can, on the other hand, be extracted by proper interplay of experiment and theory.

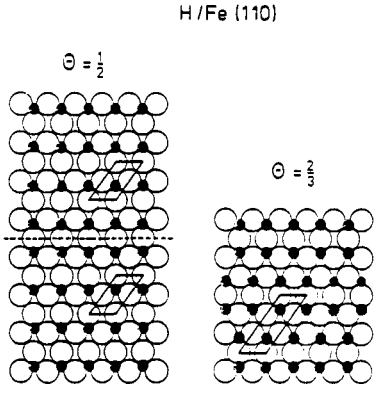

Fig. 7: Ordered structures (2x1 and 3x1) formed by chemisorbed H atoms on a Fe(110) surfact at low temperature.

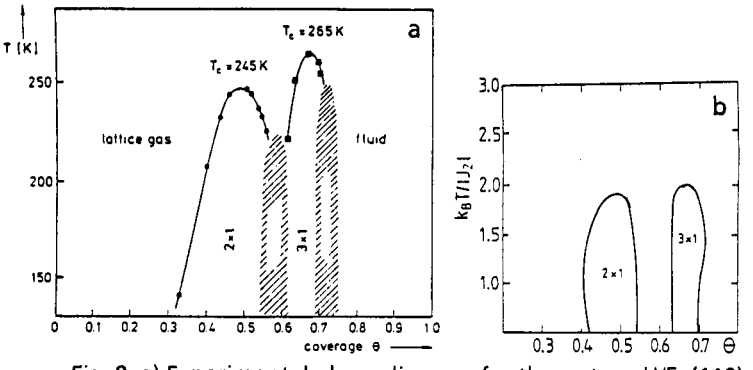

Fig. 8: a) Experimental phase diagram for the system H/Fe(110)
b) Theoretical phase diagram (ref. 10)

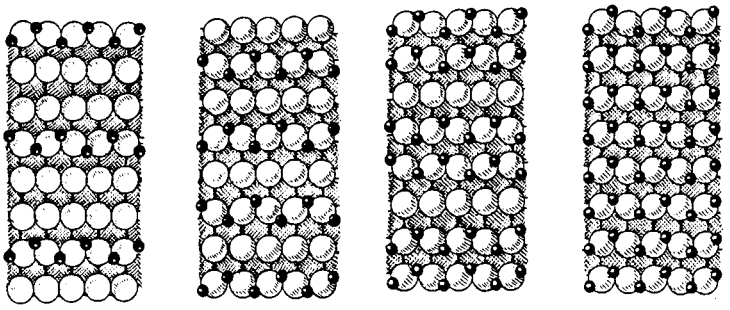

Fig. 9: Lattice gas structures formed by H atoms chemisorbed on a Ni(110) surface below 180 K at $\Theta = 1/3$, 1/2, 2/3 and 1, respectively.

Another example for the formation of lattice-gas structures is presented by the system H/Ni(110) for temperatures below 180 K. As can be seen from fig. 9 up to $\Theta = 1$ a whole series of ordered structures form in which the H-atoms form always 'zig-zag' rows along the [110]-direction, while the spacing along the [001]-direction between parallel rows varies with coverage (ref. 11). At $\Theta = 1$ all H-atoms are located in three-fold coordinated sites on a laterally undistorted substrate lattice (ref. 12). This situation does, however, not represent the saturation coverage, but the surface may take up additional H-atoms up to $\Theta = 1.5$. This process proceeds as a first-order phase transition in that islands of the new 1x2-phase (with local coverage 1.5) grow at the expense of the fraction of the total surface area being present as the 1x1-phase with $\Theta = 1.0$. The structure of the 1x2-phase is of the type as illustrated in fig. 10 (ref. 13): Parallel rows of Ni atoms are laterally displaced (row pairing). This reconstruction of the surface not only involves the Ni atoms from the topmost layer, but is also associated with 'buckling' of the atoms within the second layer. (It should be noted that in this case the actual positions of the H-atoms cannot be determined precisely, however, there exists fairly high accuracy with respect to the configurations of the Ni atoms). The driving force for this transformation of the surface structure has to be sought in the gain in free energy by the occupation of additional adsorption sites created by the reconstruction which overcompensates the increase of free energy associated with this process. The fact that this transformation occurs even at 110 K without any noticeable activation energy demonstrates how unstable the structure of a metal surface may be under the influence of an adsorbate.

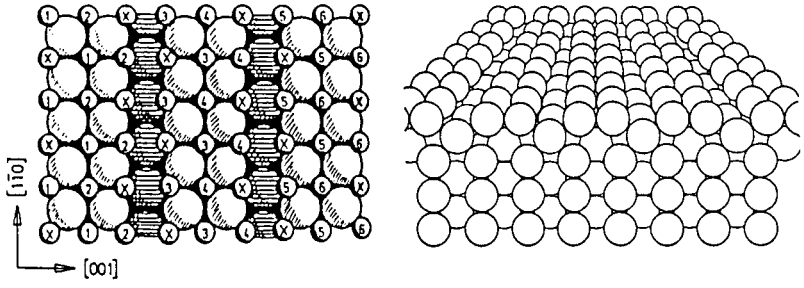

Fig. 10: Structure of the reconstructed ('row-pairing') 1x2-phase on Ni(110) with a H-coverage of $\Theta = 1.5$. The perspective view (right) shows only the Ni atoms.

Also the opposite effect is observed in a number of aces: The structure of a clean surface is reconstructed because of its lower surface free energy, but is tranformed into the 'normal' (unreconstructed) configuration under the influence of an adsorbate. An example of this type is offered by the system CO/Pt(100): The atoms of the topmost layer of a clean, stable Pt(100) surface form a quasi-hexagonal ('hex') arrangement instead of the square configuration corresponding to the bulk termination (1x1) (ref. 14). As illustrated schematically by fig. 11 (ref. 15) this is due to the fact that the clean hex-surface is energetically more stable than the clean-1x1 surface. The heat of CO adsorption on the (metastable) 1x1-phase is, on the other hand, about 40 kJ/mol larger than on the hex-surface. As a consequence, through a first-order phase transformation patches of the 1x1-surface with local-CO-coverage of 0.5 (c2x2-phase) are formed without noticeable activation energy as soon as the average CO coverage on the hex-surface exceeds a critical value of about $\Theta = 0.05$-0.08 (refs. 15,16). The reverse transformation, 1x1→hex, starts when the CO-coverage on the 1x1-phase drops below another critical value of about 0.3 (refs. 15,16), and if the temperature is high enough (>400 K) to overcome the activation barrier $E^* \approx 100$ kJ/mol (ref. 17). Because these first-order phase transitions are associated with nucleation-growth phenomena no true adsorption-desorption equilibrium but rather pronounced hysteresis effects are observed with this system (refs. 15,16): As can be seen from fig. 12, depending on whether the temperature is rised or lowered in a constant CO pressure, over a certain range either a high or a low CO coverage is observed. It is quite obvious, that mere macroscopic measurements of adsorption isotherms would never be able to provide a satisfactory explanation of such phenomena.

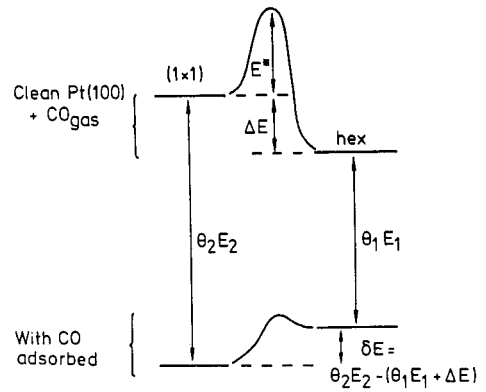

Fig. 11: Schematic energy diagram for the two modifications of the Pt(100) surface (hex and 1x1) under the influence of CO adsorption.

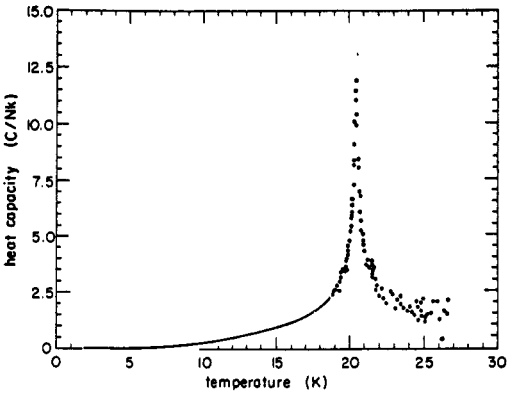

Fig. 13: Heat capacity of a para-H_2 monolayer on graphite signaling a commensurate solid/disordered-fluid phase transition (ref. 20a).

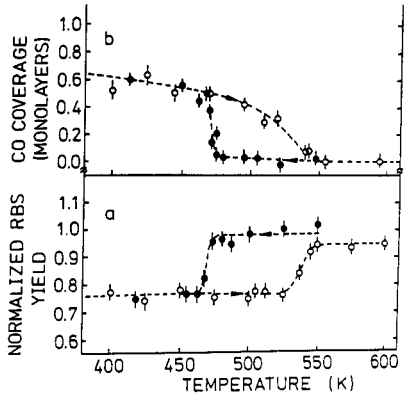

Fig. 12: Hysteresis effects upon slow heating or cooling of a Pt(100) surface in a CO atmosphere of p = 6.7x10-5 Pa (ref. 16)
a) Rutherford backscattering spectroscopy (RBS) data reflecting the presence of the 1x1 (low yield) or the hex (high yield) surface structure.
b) CO coverage as determined by nuclear microanalysis.

PHYSISORPTION

Due to the much weaker adsorbate-surface interaction in physisorption which may become comparable to the adsorbate-adsorbate interaction, the equilibrium between gas and solid will generally not be confined to the first monolayer but may also include the formation of multilayers and finally complete condensation. Again the conditions may be chosen in a similar way as before, in that the rate of desorption is negligible and only the equilibrium within the first monolayer (without gas phase) is studied. The general structural features of these physisorbed phases bear some resemblance to those of the CO chemisorption layers discussed above. At low coverages commensurate phases are formed, while near monolayer completion incommensurate structures appear which reflect the competition between adsorbate-adsorbate and adsorbate-substrate interactions.

Very detailed investigations (both experimentally and theoretically) on the thermodynamic and structural properties of such phases, mainly adsorbed on graphite but also on metal single crystal surfaces, have been performed during the past years (ref. 18), and a comprehensive treatment of these phenomena would go far beyond the limits of this short contribution. To pick up just a single example, we mention the rich variety of phases detected by LEED and neutron scattering of H_2 and D_2 on graphite (ref. 19) whose phase transitions are also reflected in corresponding heat capacity data (ref. 20, cf. fig. 13).

The BET isotherm represents the most popular description of the gas-surface equilibrium in physisorbed systems which is an extension of the Langmuir concept to multilayer adsorption (ref. 21). Although the monolayer capacity is assumed to be determined by dense packing of the adsorbed particles, their mutual interactions are again neglected. In addition, it is assumed that the adsorption energy for the second monolayer is equal to those of all higher layers, but differs from that of the first monolayer. Fig. 14 shows the isosteric heat of adsorption of Xe on a Pd(100) surface with regular monoatomic steps as a function of coverage (ref. 22) which by no means agrees with these assumptions: At very low coverages the step sites are occupied which exhibit the largest adsorption energy. Within the first monolayer E_{ad} decreases continuously due to the operation of dipole-dipole repulsions, as reflected by the marked change of the work function. There is then a drop in E_{ad}, which remains constant over the second monolayer for which the van der Waals attractions between the adsorbed Xe atoms overcompensate their dipole-dipole repulsion and cause two-dimensional condensation. The adsorption energy for the third layer is still lower, and only then remains constant (within the limits of accuracy) and equal to the heat of sublimation.

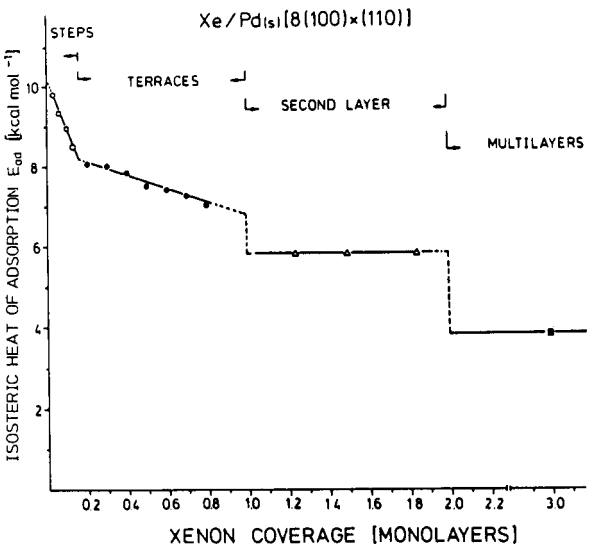

Fig. 14: Isosteric heat of adsorption for Xe on a stepped Pd(100) surface.

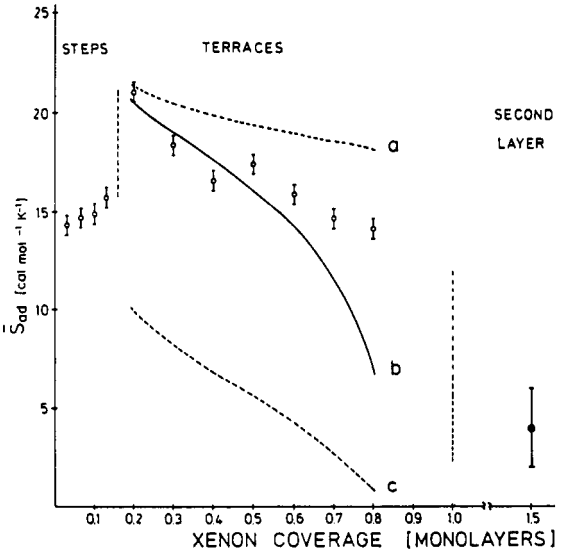

Fig. 15: Differential entropy of adsorption for Xe on a stepped Pd(100) surface.

The differences in the state of adsorption with coverage are to some extent also reflected in the differential entropy of adsorption as reproduced in fig. 15. For the initial adsorption at step sites, S_{ad} has a rather constant value of ~60 kJ/mol·K. When occupation of the terrace site starts, there is a noticeable increase in entropy (reflecting higher mobility), followed by continuous decrease. In this range of the first monolayer the experimental data are between theoretical values for a completely mobile 2D ideal gas (curve a) and for a localized overlayer (curve c), but close to the predictions for mobile Volmer gas which takes the size of the Xe atom into account (curve b).

As a consequence of the BET model the $(n+1)^{th}$ layer starts to form already before the n^{th} layer is completed, which leads to smooth isotherms without any discontinuities. Studies with energetically homogeneous surfaces at low enough temperatures reveal that this is by no means the case, but that steplike isotherms may be found signaling layer-by-layer condensation (ref. 24). A series of isotherms for the Xe/Pd(100)-s system is reproduced in fig. 16 (ref. 23) which exhibit, at low enough temperatures, pronounced steps marking first-order phase transitions after completion of the first, second and third monolayer. Only above 68 K the isotherms become smoother and suggest e.g. the onset of the formation of the third monolayer before the second one is completed. In this case the use of ultraviolet photoelectron spectroscopy (UPS) enabled even direct determination of the equilibrium populations of the individual layers as function of pressure and temperature. The resulting data are reproduced in fig. 17 in the form of histograms and demonstrate indeed that up to ~68 K the layers are successively populated, while above this temperature the third layer already starts to become partly occupied before the second layer is completed. This example represents experimental verification of a 'roughening transition' for the case of gas-solid equilibrium, for which the theory was originally developed in the field of crystal growth (ref. 25) and which received particular attention in recent years (ref. 26).

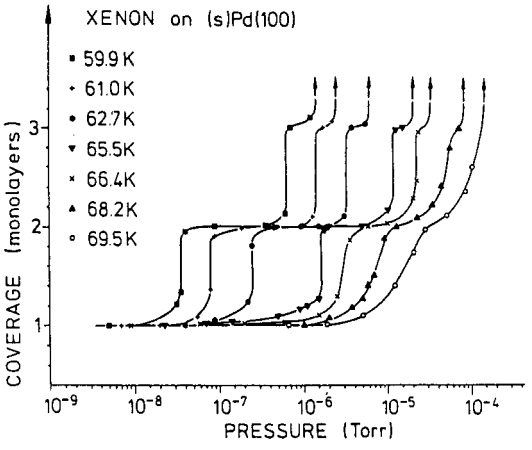

Fig. 16: Adsorption isotherms for Xe on a stepped Pd(100) surface at various temperatures.

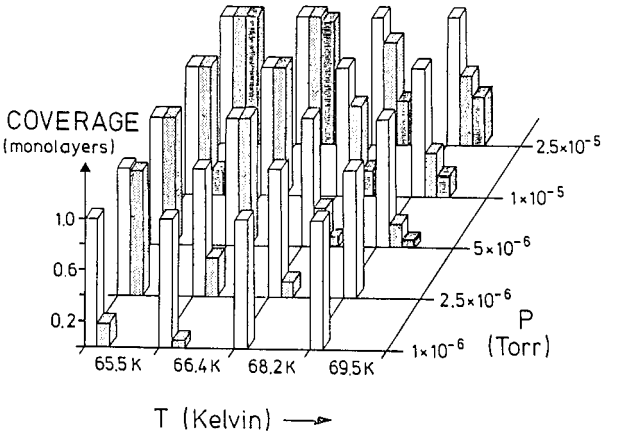

Fig. 17: Histograms for the populations of different layers in the system Xe/Pd(110)-s at different temperatures and pressures.

CONCLUSIONS

Only a few selected examples could be presented in order to illustrate the rich variety of gas-solid interaction phenomena. Application of surface physical methods in combination with the concepts of thermodynamics to well-defined single crystal surfaces as model systems permit detailed insights into their microscopic processes and understanding of the resulting macroscopic properties. The latter are of course also of tremendous importance with 'real' systems, not only with respect to gas adsorption but also in hetereogeneous catalysis, where the chemical equilibrium between gaseous compounds is approached through intermediate chemisorption steps.

REFERENCES

1. a) G. A. Somorjai, Chemistry in two dimensions: Surfaces, Cornell Univ. Press. (1981).
   b) G. Ertl and J. Küppers, Low energy electrons and surface chemistry, 2nd ed., Verlag Chemie, Weinheim (1985).
   c) D. P. Woodruff and T. A. Delchar, Modern Techniques of Surface Science, Cambridge Univ. Press (1986).
2. See, e.g. A. W. Adamson, Physical Chemistry of Surfaces, 3rd ed., p. 553, Wiley, New York (1976).
3. I. Langmuir, J. Am. Chem. Soc., 40, 1361 (1918).
4. G. Ertl and J. Koch, Z. Naturforsch., 25a, 1906 (1970).
5. a) H. Conrad, G. Ertl and J. Küppers, Surf. Sci., 76, 323 (1978).
   b) A. M. Bradshaw and F. M. Hoffmann, Surf. Sci., 72, 513 (1978).
6. See for example: a) E. Shustorovich, Surf. Sci. Rep., 6, 1-63 (table 6) (1986).
   b) K. Christmann, Surf. Sci. Rep., 9, 1-163 (ch. 2.9) (1988).
7. R. J. Behm, K. Christmann, G. Ertl and M. A. Van Hove, J. Chem. Phys., 73, 2984 (1980).
8. T. L. Einstein, CRC Crit. Rev. Solid State Mater. Sci., 7, 261 (1978).
9. a) R. Imbihl, R. J. Behm, K. Christmann, G. Ertl and T. Matsushima, Surface Sci., 117, 257 (1982).
   b) W. Moritz, R. Imbihl, R. J. Behm, G. Ertl and T. Matsushima, J. Chem. Phys., 83, 1959 (1985).
10. a) W. Kinzel, W. Selke and K. Binder, Surface Sci., 121, 13 (1982).
    b) W. Selke, W. Binder and W. Kinzel, Surface Sci., 125, 74 (1983).
11. a) T. Engel and K. H. Rieder, Surface Sci., 109, 140 (1981).
    b) V. Penka, K. Christmann and G. Ertl, Surface Sci., 136, 307 (1984).
12. W. Reimer, V. Penka, M. Skottke, R. J. Behm, G. Ertl and W. Moritz, Surface Sci., 186, 45 (1987).
13. G. Kleinle, V. Penka, R. J. Behm, G. Ertl and W. Moritz, Phys. Rev. Lett., 58, 148 (1987).
14. a) P. Heilmann, K. Heinz and K. Müller, Surface Sci., 83, 487 (1979).
    b) M. A. Van Hove, R. J. Koestner, P. C. Stair, J. P. Biberian, L. L. Kesmodel, I. Bartos and G. A. Somorjai, Surface Sci., 103, 189 (1981).
15. R. J. Behm, P. A. Thiel, P. R. Norton and G. Ertl, J. Chem. Phys., 78, 7437; 7448 (1983).
16. T. E. Jackman, K. Griffiths, J. A. Davies and P. R. Norton, J. Chem. Phys., 79, 3529 (1983).
17. a) P. R. Norton, J. A. Davies, D. K. Creber, C. W. Sitter and T. E. Jackman, Surface Sci., 108, 205 (1981).
    b) K. Heinz, E. Lang, K. Strauss and K. Müller, Appl. Surf. Sci., 11/12, 611 (1982).
18. a) S. K. Sinha (ed.), Ordering in two dimensions, Elsevier, New York (1980).
    b) J. G. Dash and J. Ruvalds (Eds.), Phase Transitions in Surface Films, Plenum Press, New York (1980).
    c) Ber. Bunsenges. Phys. Chem., 90, 184-316 (1986).
19. a) M. Nielsen, J. D. McTague and L. Passell, in ref. 18b), p. 127.
    b) J. Cui and S. C. Fain, Jr., Phys. Rev. B, (submitted).
    c) J. Cui, S. C. Fain, Jr., H. Freimuth, H. Wiechert, H. P. Schildberg and H. J. Lauter, Phys. Rev. Lett., 60, 1848 (1988).
20. a) F. C. Mottler and J. G. Dash, Phys. Rev. B31, 346 (1985).
    b) H. Freimuth and H. Wiechert, Surface Sci., 162, 432 (1985); 178, 716 (1986).
21. S. Brunauer, P. H. Emmett and E. Teller, J. Am. Chem. Soc., 60, 309 (1938).
22. R. Miranda, S. Daiser, K. Wandelt and G. Ertl, Surface Sci., 131, 61 (1983).
23. R. Miranda, E. V. Albano, S. Daiser, K. Wandelt and G. Ertl, J. Chem. Phys., 80, 2931 (1984).
24. A. Thomy, X. Duval and J. Regnier, Surf. Sci. Rep., 1, 1 (1981).
25. R. W. Burton, N. Cabrera and F. C. Frank, Phil. Trans. R. Soc. London, A243 , 229 (1951).
26. a) J. D. Weeks and G. Gilmer, Adv. Chem. Phys., 40, 157 (1979).
    b) Y. Larher, this conference.